Papathanassiou and Davydov *EURASIP Journal on Wireless Communications and Networking* 2011, **2011**:63
http://jwcn.eurasipjournals.com/content/2011/1/63

EURASIP Journal on
Wireless Communications and Networking
a SpringerOpen Journal

RESEARCH Open Access

The promise of downlink MU-MIMO for high-capacity next generation mobile broadband networks based on IEEE 802.16 m

Apostolos Papathanassiou* and Alexei Davydov

Abstract

The dramatic increase of the demand for mobile broadband services poses stringent requirements on the performance evolution of currently deployed mobile broadband networks, such as Mobile WiMAX Release 1 and 3GPP LTE Release 8. Although the combination of single-user multiple-input multiple-output (SU-MIMO) and orthogonal frequency division multiple access (OFDMA) provide the appropriate technologies for improving the downlink performance of third generation (3G) code division multiple access (CDMA)-based mobile radio systems and, thus, address the current mobile internet requirements, a fundamental paradigm shift is required to cope with the constantly increasing mobile broadband data rate and spectral efficiency requirements. Among the different technologies available for making the paradigm shift from current to next-generation mobile broadband networks, multiuser MIMO (MU-MIMO) constitutes the most promising technology because of its significant performance improvement advantages. In this article, we analyze the performance of MU-MIMO under a multitude of deployment scenarios and system parameters through extensive system-level simulations which are based on widely used system-level evaluation methodologies. The target mobile broadband system used in the simulations is IEEE 802.16 m which was recently adopted by ITU-R as an IMT-Advanced technology along with 3GPP LTE-Advanced. The results provide insights into different aspects of MU-MIMO with respect to system-level performance, parameter sensitivity, and deployment scenarios, and they can be used by the mobile broadband network designer for maximizing the benefits of MU-MIMO in a scenario with specific deployment requirements and goals.

1. Introduction

Current mobile traffic usage based on the operators' and the analysts' reports [1] as well as forecasts on mobile data traffic growth [1,2] indicates that mobile networks will have to fulfill even more stringent spectral efficiency requirements in the next 4-5 years. Although fourth generation (4G) mobile broadband networks such as Mobile WiMAX Release 1 and 3GPP LTE Release 8 more than double the spectral efficiency of third generation (3G) cellular networks, further technological advances need to be available to mobile operators to satisfy the mobile broadband service demand of their users. The spectral efficiency improvement of 4G mobile broadband networks is due to the combination of multiple-input multiple-output (MIMO) techniques with orthogonal frequency division multiple access (OFDMA) which allows a significantly more efficient spectrum usage compared to code division multiple access (CDMA)-based 3G networks. However, the flavor of MIMO used in current 4G deployments is termed single-user MIMO (SU-MIMO) and allows the base station (BS) transmitter to transmit only to a single user at a time. This means that the data rate performance strongly depends on the mobile broadband channel condition of the user: The data rate of the considered user can increase only if the channel condition allows for the transmission of more than one data streams, i.e., only if the so-called channel rank is high [3]. Unfortunately, the probability of transmitting more than one data stream to the same user, termed as spatial multiplexing (SM), rarely exceeds 20% in typical 4G network deployments even with advanced MIMO receivers [4,5]. As it is

* Correspondence: apostolos.papathanassiou@intel.com
Wireless Technology Division, Mobile Wireless Group, Intel Architecture Group, Intel Corporation, Santa Clara, USA

shown in [6], the situation does not improve sufficiently by employing beamforming (BF) techniques with more transmit antennas, e.g., four instead of two, at the BS. Multiuser MIMO (MU-MIMO) has been shown to overcome the deficiencies of SU-MIMO by allowing for multiplexing data streams from multiple users rather than multiplexing multiple data streams from a single user. In this way, MU-MIMO turns the fundamental problem of SU-MIMO with low-rank channels into an advantage [3]. Furthermore, unlike SU-MIMO system operation, multiplexing the appropriate set of users based on criteria such as the inter-user BF–also referred to as spatial signature [3]–correlation factors can lead to additional gains if more transmit antennas are used at the BS. For more information on MU-MIMO, the reader is referred to [7-10] and the references therein.

Despite the significant advantages of MU-MIMO for next-generation mobile broadband communications, there are challenges regarding the deployment and operation of MU-MIMO in practical networks. This article analyzes the performance of MU-MIMO under a multitude of deployment scenarios and system parameters through extensive system-level simulations which are based on two widely used system-level evaluation methodologies: The IMT-Advanced evaluation methodology [11] and the IEEE 802.16 m evaluation methodology [12]. The use of two evaluation methodologies provides different views on mobile broadband deployment models which are expected to increase the probability of good correlation with real-world deployment scenarios. The target mobile broadband system used in the simulations is IEEE 802.16 m [13] which is the evolution of IEEE 802.16e–the standard basis for Mobile WiMAX Release 1–and employs MU-MIMO as the core technology for achieving significant performance gains over its predecessor. It is worth noting that IEEE 802.16 m was recently adopted by ITU-R as an IMT-Advanced technology together with 3GPP LTE-Advanced.

The IEEE 802.16 m standard supports both open-loop (OL) and closed-loop (CL) MIMO modes. In the case of SU-MIMO, OL SU-MIMO is supported for 2, 4, and 8 transmit antennas for transmit diversity and SM. CL SU-MIMO using codebook-based precoding is supported for FDD and TDD. IEEE 802.16 m allows for the use of transformed codebook which improves the BF performance by filtering the selected codebook index at the mobile station (MS) by the long-term covariance matrix of the channel between the MS and its serving sector. In the case of TDD, uplink (UL) sounding can also be employed for sounding-based precoding because of the downlink and UL channel reciprocity in TDD. In the case of MU-MIMO, two transmit antennas can support up to two streams and users, while four and eight transmit antennas can support up to four streams and users.

The results in this article provide insights into different aspects of MU-MIMO with respect to system-level performance, parameter sensitivity, and deployment scenarios. Although the investigations of the different dependencies in MU-MIMO are not exhaustive–neither with respect to the deployment scenarios nor with respect to the parameter sensitivities, the results and analysis in the article can be used by the mobile broadband network designer for maximizing the benefits of MU-MIMO in a scenario with specific deployment requirements and goals. The rest of this article is organized as follows: Section 2 describes the system-level simulation assumptions providing details on the evaluation methodologies, system configuration, simulation flow, and control overhead calculation. Section 3 analyzes the dependence on the evaluation methodologies and Section 4 analyzes the dependence on representative deployment parameters such as deployment scenarios and antenna configuration. Section 5 deals with the impact of main system parameters, such as duplex mode, permutations, amount of MS feedback, and estimation and signaling errors, on the performance of MU-MIMO. Section 6 provides an overview of the high-performance technology evolution enabled by MU-MIMO in the example of the IEEE 802.16e and IEEE 802.16 m mobile broadband systems. Section 7 summarizes the main results and concludes the article.

2. Simulation assumptions

This section contains the background information necessary for generating the results presented in Sections 3-6. After referring to the mobile broadband system-level evaluation methodologies used for generating the results of this article, the main system configuration parameters for IEEE 802.16 m are described. Then, the system-level simulation flow is presented to give a more detailed view on the overall system operation including the details of the MU-MIMO functionality. Finally, control overhead calculation issues are addressed for shedding more light on the control signaling portion of the system operation and its impact on the spectral efficiency calculation.

2.1. Evaluation methodologies

In order to provide system-level simulation results which can be utilized in the most effective way, the well-known and widely adopted mobile broadband evaluation methodologies are used throughout the article. More specifically, the IMT-Advanced evaluation methodology as described in Report ITU-R M.2135-1 [11] and the IEEE 802.16 m evaluation methodology as described in document IEEE 802.16 m-08 [12] are adopted for evaluating

the performance of MU-MIMO for the target IEEE 802.16 m mobile broadband system.

The IMT-Advanced evaluation methodology was developed by ITU-R WP (Working Party) 5D to provide guidelines for evaluating the proposed IMT-Advanced candidate technologies. Although the IMT-Advanced evaluation process in ITU-R has been completed, it is expected that the IMT-Advanced evaluation methodology will be widely used as the basis for evaluating mobile broadband systems beyond IMT-Advanced in the years to come. In this article, the three mandatory test environments of the IMT-Advanced evaluation methodology with a hexagonal layout are simulated. The main parameters of each test environment are shown in Table1 [11]. As shown in Table 1, the considered test environments of the IMT-Advanced evaluation methodology span a wide range of mobile broadband deployment scenarios regarding cell size, channel model, carrier frequency, and user speeds.

The IEEE 802.16 m evaluation methodology was developed by IEEE 802.16 m Task Group M to define guidelines and criteria for the evaluation of proposed concepts during the standardization of IEEE 802.16 m. Since the IEEE 802.16 m evaluation methodology contains both Mobile WiMAX Release 1 and IEEE 802.16 m specific elements, it is used in this article for evaluating the performance of the considered IEEE 802.16 m mobile broadband system and compare it with its predecessor in Section 7. To enable a mapping between the investigated IMT-Advanced test environments, see Table 1, and the baseline test scenario of the IEEE 802.16 m evaluation methodology, see Table three of [12], the simulation results for the IEEE 802.16 m evaluation methodology are usually presented separately for the three individual channel models and user speeds of the baseline test scenario, i.e., ITU Pedestrian B channel model with 3 km/h user speed (ITU PB3), ITU Vehicular A channel model with 30 km/h user speed (ITU VA30), and ITU Vehicular A channel model with 120 km/h user speed (ITU VA120). Certainly, the combined results–also referred to as mixed mobility results–are also presented for the IEEE 802.16 m evaluation methodology when necessary, e.g., see Section 7.

2.2. System configuration

In this section, we provide the assumptions of the IEEE 802.16 m mobile broadband system used in the simulations for evaluating the performance of MU-MIMO. The main OFDMA and frame parameters of IEEE 802.16 m are listed in Table 2 of the Appendix in this article, see also [13] and the companion documents [14,15]. Following the IMT-Advanced guidelines, the parameter values in Table 2 of the Appendix are shown for both time division duplex (TDD) and frequency division duplex (FDD) modes of IEEE 802.16 m in case they differ. Table 3 of the Appendix in this article lists the main downlink system parameters of IEEE 802.16 m according to [13-16].

According to Table 3 of the Appendix, it is emphasized that there is a synergy between the used subchannelization scheme and the multi-antenna transmission format which directly defines the feedback requirements from the MS to the BS: in the case of contiguous permutations–referred to as subband logical resource unit (SLRU) in IEEE 802.16 m–which facilitate the application of frequency-selective scheduling, MU-MIMO transmissions are allocation dependent and, thus, require narrowband (subband-based) channel quality indicator (CQI) and transformed codebook index (TCI) feedback from the MS. In the case of distributed permutations–referred to as miniband logical resource unit (NLRU) in IEEE 802.16 m–which maximize the frequency diversity in the DL, MU-MIMO transmissions are allocation independent and, thus, require wideband CQI and long-term preferred matrix index (LT-PMI) feedback from the MS, i.e., a single CQI and LT-PMI value is sufficient for obtaining the benefits from diversity transmission. Alternatively, the LT-PMI can be replaced by the quantized long-term covariance matrix (LT-CM) in the case of NLRU [13,16]. Therefore, the reference to the use of SLRU or NLRU permutations explicitly defines the multi-antenna transmission format and the feedback from the MS to the BS. Independently from the use of SLRU or NLRU permutations, the overall MU-MIMO operation is similar for both SLRU and NLRU which significantly facilitates the implementation of MU-MIMO-based transceivers in next-generation mobile broadband systems like IEEE 802.16 m. The details of the MU-MIMO pairing process are described in Section 2.3 in conjunction with the overall system operation and simulation.

Table 1 Main parameters of the four mandatory IMT-Advanced test environments

	Urban microcell (UMi)	Urban macrocell (UMa)	Rural macrocell (RMa)
Layout	Hexagonal grid	Hexagonal grid	Hexagonal grid
Inter-site distance	200 m	500 m	1732 m
Channel model	Urban micro model	Urban macro model	Rural macro model
Carrier frequency	2.5 GHz	2 GHz	800 MHz
User speed	3 km/h	30 km/h	120 km/h

Table 2 Main OFDMA and frame parameters of IEEE 802.16 m

Parameter	Description	Value	
		TDD	FDD
BW	Total bandwidth	20 MHz	2 × 10 MHz
N_{FFT}	Number of points in full FFT	2048	1024
F_s	Sampling frequency	22.4 MHz	11.2 MHz
Δ_f	Subcarrier spacing	10.9375 kHz	
$T_o = 1/\Delta_f$	OFDMA symbol duration without cyclic prefix	91.43 μs	
CP	Cyclic prefix length (fraction of T_0)	1/16	
T_s	OFDMA symbol duration with cyclic prefix	97.143 μs	
T_f	Frame length	5 ms	
N_F	Number of OFDMA symbols in frame (excluding switching gaps)	50	51
R_{DL-UL}	Ratio of DL to UL	Five DL subframes, three UL subframes	Eight DL subframes for DL and UL
T_{duplex}	Duplex time	TTG + RTG = 165.71 μs	N/A

2.3. Simulation flow

In this section, the simulation flow is presented to facilitate the understanding of the system operation for a mobile broadband system such as IEEE 802.16 m including the MU-MIMO functionality. The simulation flow is shown in Figure 1 and consists of a number of steps which are defined by each separate box in Figure 1.

In a first step, the initialization phase takes place which is mostly related to the initialization of different statistics-bearing structures used in the different steps of the simulation. After all the structures are initialized, the hexagonal layout is generated which is the geographic placement of the BS network nodes. Then, the wrap-around cellular deployment model (see [12] for a detailed description) and the generation of the large-scale parameters (LSPs), such as pathloss and shadowing models as well as their correlation, take place. While the wrap-around model is the same for both evaluation methodologies considered in this article, the information related to the LSPs depends on the evaluation methodology: although the IEEE 802.16 m evaluation methodology specifies a single pathloss and shadowing model for all the user speed scenarios of 3, 30, and 120 km/h [12], the IMT-Advanced evaluation methodology defines different pathloss and shadowing models for UMi, UMa, and RMa [11]. The difference in the LSPs implies that after a user is uniformly dropped in the network and cell selection takes place, which refers to the assignment of each user to a serving sector according to the maximum received power criterion, the calculation of the geometry, which is the long-term signal-to-interference-plus-noise ratio (SINR) per user in the network, leads to different SINR distributions depending on the evaluation methodology. This fact is illustrated in Section 3 where the impact of the evaluation methodology on the system-level performance of MU-MIMO is investigated.

After the long-term statistics are available, the execution of the short-term, frame-based steps is initiated. There are three major tasks that are executed on a per-frame basis in the simulations: MS feedback calculation and transmission to the BS, scheduling of user transmissions, and DL transmission.

As the first major task, the feedback for CQI and TCI in the case of SLRU or LT-PMI/LT-CM in the case of NLRU needs to be calculated for each MS in the network. To accomplish this task, the channels–also referred to as channel impulse responses (CIRs)–corresponding to the links among each MS and its serving and interfering sectors in the network are generated. The complexity of this simulation step is significantly reduced because the required channels need to be generated only for the DL sounding OFDMA symbol, termed as Advanced Midamble (A-MIDAMBLE) in IEEE 802.16 m, and not for all OFDMA symbols in the DL portion of the frame in the case of TDD operation or in the DL frame in the case of FDD operation. After determining the TCI or LT-PMI/LT-CM feedback, the calculation of the CQI explicitly accounts for the BF gain achieved using the selected TCI or LT-PMI/LT-CM information. The determination of the TCI feedback for SLRU or LT-PMI feedback for NLRU relies on the maximization of the channel capacity with the channel being the average CIR per subband in the case of SLRU or the wideband CIR in the case of NLRU. When the TCI is calculated, filtering with the LT-CM is also performed as prescribed by the IEEE 802.16 m standard [3]. The calculation of the CQI is based on the post-processing SINR for an MMSE receiver and utilizes either a single BF vector in the case of TCI and LT-PMI or the singular vector corresponding to the largest singular value of the quantized signal covariance matrix in the case of LT-CM; in the latter case, the calculation of an $M \times M$ singular value decomposition (SVD) is implied where M represents

Table 3 Main downlink parameters of IEEE 802.16 m [16]

Topic	Description	IEEE 802.16 m parameter
Basic modulation for data	Modulation schemes for data	QPSK, 16QAM, 64QAM
Basic modulation for control	Modulation schemes for control	QPSK
Duplexing scheme	TDD or FDD	TDD/FDD
Subchannelization for data	Contiguous/Distributed Resource Units and permutations	- Subband LRU (SLRU) as defined in Sections 15.3.5.1-15.3.5.3 of [3]; 12 equal-size allocations spanning the complete duration of the time resources (DL portion of the TDD frame, DL FDD frame) NLRU as defined in Sections 15.3.5.1-15.3.5.3 of [3]; 6 equal-size allocations spanning the complete duration of the time resources (DL portion of the TDD frame, DL FDD frame)
Subchannelization for control	Contiguous/distributed resource units and permutations	DLRU as defined in Sections 15.3.5.1-15.3.5.3 of [3]
Downlink Pilot Structure	Pilot structure, density etc.	Depends on the number of streams per allocation:1, 2, 3, and 4 pilot streams as defined in Section 15.3.5.4.1 of [3]; 2 dB pilot power boosting for 1, 2 streams and 0 dB power boosting for 3, 4 streams
Multi-antenna Transmission Format for data	Multi-antenna configuration and transmission scheme	- In the case of SLRU:6-bit transformed codebook; adaptive switching among one stream SU-MIMO, two stream MU-MIMO, three stream MU-MIMO and four stream MU-MIMO In the case of NLRU: long-term BF by using the quantized long-term covariance matrix or wideband PMI; adaptive switching among one stream SU-MIMO, two stream MU-MIMO, three stream MU-MIMO and four stream MU-MIMO
Multi-antenna transmission format for A-A-MAP	Multi-antenna configuration and transmission scheme	OL SFBC + non-adaptive precoding ($T_x$diversity)
Receiver structure	Receiver interference awareness	MMSE for both channel estimation and data detection
Data channel coding	Channel coding schemes	Convolutional turbo coding (CTC) 1/3
Control channel coding for A-A-MAP	Channel coding schemes and block sizes	As described in Section 15.3.6.3.2.2 of [3] with MLRU size equal to 56 tones
Scheduling	Demonstrate performance/fairness criteria in accordance to traffic mix	Proportional Fair for full buffer data
Link adaptation	Modulation and coding schemes (MCS), CQI feedback delay/error	Choice of 16 MCS schemes inclusive of coding rate and rate matching, see Section 15.3.12.1.2 of [3]
Link to system mapping	MI-based PHY abstraction	MMIB PHY abstraction [2]
HARQ	HARQ transmission specifics	Chase Combining Asynchronous, adaptive, 3 subframe ACK/NACK delay, maximum 4 HARQ retransmissions, minimum retransmission delay 3 subframes
Interference model	Co-channel interference model, fading model for interferers, number of major interferers, threshold	Explicitly modeled Average interference on used subcarriers per LRU (subband or miniband) in PHY abstraction
Control signaling	Message/signaling format, overheads	Signaling errors were modeled for A-A-MAP and HF-A-MAP and sounding estimation errors were modeled for A-MIDAMBLE
Control channel overhead	L1/L2 Overhead	Dynamic overhead modeling for A-A-MAP and HF-A-MAP and fixed overhead modeling for non-user specific A-MAP (NUS-A-MAP), A-PREAMBLE, A-MIDAMBLE, and SFH

the number of transmit ($T \times$) antennas at the BS transmitter. It is emphasized that the feedback information is generated assuming single data stream or rank-1 transmission. The BS scheduler is responsible for making the necessary CQI adjustments depending on MU-MIMO and hybrid automatic repeat request (HARQ) related criteria as it will be discussed later in this section. After the feedback information is available, transmission to the BS is simulated by assuming a fixed UL error rate value which is calculated from UL control channel simulations. MS feedback is transmitted every 5 ms (one frame) for CQI, TCI, and LT-PMI; the LT-CM is fed back every 20 ms (four frames). Finally, it is noted that the MS feedback is appropriately delayed at the BS before it is used by the BS scheduler. One frame delay is assumed between the MS feedback transmission and its usage by the BS scheduler.

As the second major task, scheduling of user transmissions at the BS takes place on a per-frame basis. In order to generate the necessary user scheduling information for MU-MIMO, the BS scheduler requires the

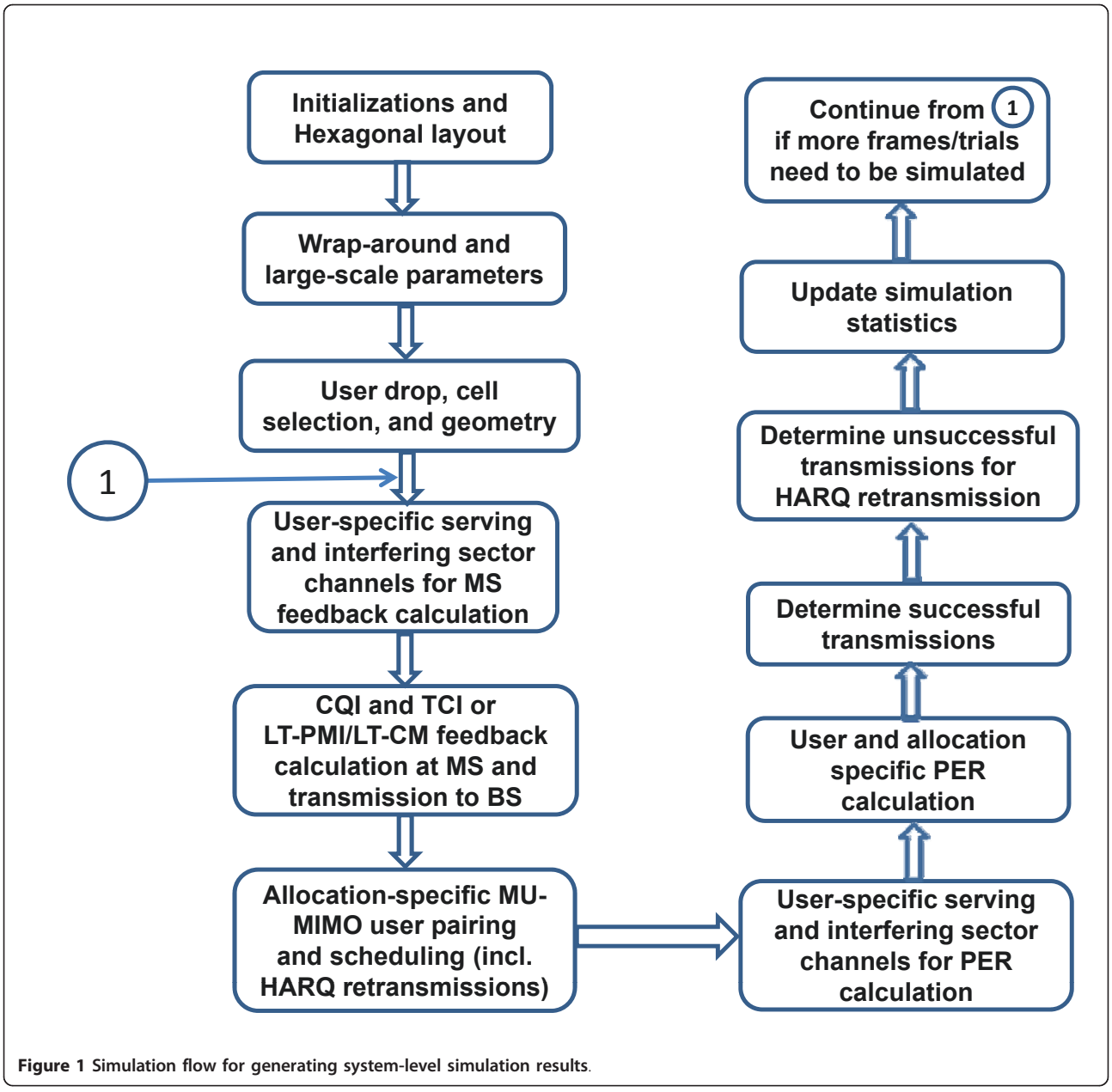

Figure 1 Simulation flow for generating system-level simulation results.

knowledge of the CQI and BF feedback from the MS–as discussed above in this section BF refers either to the TCI, the LT-PMI, or the dominant singular vector of the quantized LT-CM. The MU-MIMO scheduler operation explicitly takes into account information on HARQ. In the case that no HARQ retransmissions need to be scheduled in the current allocation, the scheduler selects the users forming a MU-MIMO set–an operation referred to as MU-MIMO pairing in the following–either through an exhaustive search among the users that can be scheduled or by selecting a number of users based on another metric, e.g., a user-specific proportional fair metric calculated independently from the MU-MIMO pairing process. Assuming zero-forcing (ZF) transmission at the BS [3,7,10], in either case the selection of the final set of users to be scheduled in the specific allocation depends on the correlation factor of the BF vectors and a joint scheduling metric which is used for prioritizing MU-MIMO user transmissions. In the simulations, a threshold-based approach is followed to determine whether two or more users are eligible for MU-MIMO pairing: If the correlation factor between the BF vectors of two users (inner product of their BF vectors) in the case of two users or all pairwise correlation factors between the BF vectors of all users in the case of more than two users are below a threshold, the

set of those users is eligible for MU-MIMO pairing; otherwise, the set of those users is excluded from scheduling in the current allocation. After all the eligible MU-MIMO sets are available, a joint scheduling metric is applied for making the final decision on the set of users to be scheduled in the current allocation. In the simulations, the sum of the individual proportional fair metrics for each MU-MIMO set is used for determining the MU-MIMO set that is scheduled in the current allocation. It is emphasized that the user-specific CQI values used in the calculation of the joint proportional fair metrics are explicitly modified due to the first step of the MU-MIMO pairing process which is based on the BF vector correlation: Since the CQI values fed back by the MS assume single-stream or rank-1 transmission, they have to be appropriately scaled to account for the fact that inter-stream interference is typically generated because of MU-MIMO transmission. In the simulations, the scaling of the CQI values is done by utilizing the BF vector information from all the users in the specific MU-MIMO set which is eligible for scheduling. The CQI values can also be subject to additional scaling according to a low-rate CQI control procedure which determines additional scaling factors according to a target packet error rate (PER) requirement and can be stream-specific, i.e., the CQI of a considered user can have different scaling factors depending on the position of the user's data stream in the MU-MIMO set. Finally, the described MU-MIMO pairing and scheduling process is essentially identical if one or more HARQ retransmissions have to be scheduled in the considered allocation. The only basic difference with the regular MU-MIMO pairing and scheduling process is related to the priority given to the allocation of as many HARQ retransmissions as possible in the considered allocation.

As the third major task following the scheduling of users in a frame, DL transmission is simulated in each sector of the mobile broadband network. For each allocation and each user, the serving and interfering sector channels are generated, which enables the calculation of user-specific post-processing SINR values and, thus, the PER for each user allocation in the network [11,12]. It is stressed that unlike the calculation of the CQI and BF feedback at the MS where only the DL sounding OFDMA symbol is sufficient, the channels for the simulation of DL transmission are generated for all OFDMA symbols in the DL portion of the frame in the case of TDD operation or in the DL frame in the case of FDD operation. Based on the calculated PER values, each user transmission is marked as successful or unsuccessful; in the latter case, the specific transmission enters the HARQ retransmission process as long as the transmission does not exceed the maximum number of allowed HARQ retransmissions. Then, the statistics-bearing structures are updated and the simulation continues to the next frame unless the maximum number of frames is reached. The simulation flow described according to Figure 1 is repeated for a number of so-called trials [11,12] to achieve converged average and cell-edge user spectral efficiency results. In the case of IEEE 802.16 m, ten trials with 500 frames per trial are typically simulated to achieve convergence of the spectral efficiency results.

2.4. Control overhead calculation

Both IMT-Advanced and IEEE 802.16 m evaluation methodologies considered in this article define the average and cell-edge user spectral efficiencies as the key output metrics of system-level evaluations [11,12]. Therefore, those two key metrics will be used throughout the article to evaluate and compare different aspects of MU-MIMO with respect to the system-level performance, parameter sensitivity, and deployment scenarios. Since the calculation of the spectral efficiency should explicitly account for the control signaling overhead [11,12], this section presents the process followed throughout the article to account for the impact of the control signaling overhead on the average and cell-edge user spectral efficiencies. As mentioned in Table 3 of the Appendix, dynamic control overhead is modeled for the Assignment-Advanced-MAP (A-A-MAP) and the HARQ Feedback-Advanced-MAP (HF-A-MAP) DL channels, and fixed control overhead is accounted for the Non-User Specific-Advanced-MAP (NUS-A-MAP), Advanced Preamble (A-PREAMBLE), Advanced Midamble (A-MIDAMBLE), and Super-Frame Header (SFH) DL channels of IEEE 802.16 m [13-16]. The following assumptions are made for each of the DL control channels of IEEE 802.16 m:

- A-A-MAP: The A-A-MAP control overhead is dynamically calculated based on the scheduler allocations in each simulated frame of both DL and UL in each deployment scenario. An A-A-MAP element is transmitted using QPSK 1/2 or QPSK 1/4; all data allocations with SINR higher than 1 dB are assigned a QPSK 1/2 A-A-MAP Information Element (IE). In the case of SLRU, up to three allocations with the same modulation and coding scheme (MCS) for a user are assigned a single A-A-MAP element; this property significantly reduces the control overhead in the case of SLRU permutations. The average DL A-A-MAP and UL A-A-MAP overhead is accounted for in the estimation of the average spectral efficiency and cell-edge user spectral efficiency.
- HF-A-MAP: The overhead calculation for the HF-A-MAP channel is based on the dynamic calculation of the required ACKs/NACKs from the UL system

level simulations for each test environment. Each HF-A-MAP channel is assumed to occupy eight tones in the A-MAP region [13].

- NUS-A-MAP: 72 subcarriers or 0.75 LRU per subframe is assumed for both TDD and FDD. According to [13], one 5-ms frame is divided into eight subframes each of 0.625 ms duration.
- A-PREAMBLE: Fixed overhead of one OFDMA symbol per 5 ms frame is assumed for both TDD and FDD.
- A-MIDAMBLE: Fixed overhead of one OFDMA symbol per 5 ms frame is assumed for both TDD and FDD.
- SFH: Fixed overhead of 20 LRUs per 20 ms superframe–equal to four 5 ms frames as defined in IEEE 802.16 m [13]–is assumed for both FDD and TDD.

In Section 3, the control overhead calculations are exemplarily shown for different deployment scenarios to clearly illustrate the impact of control signaling on the average and cell-edge user spectral efficiencies.

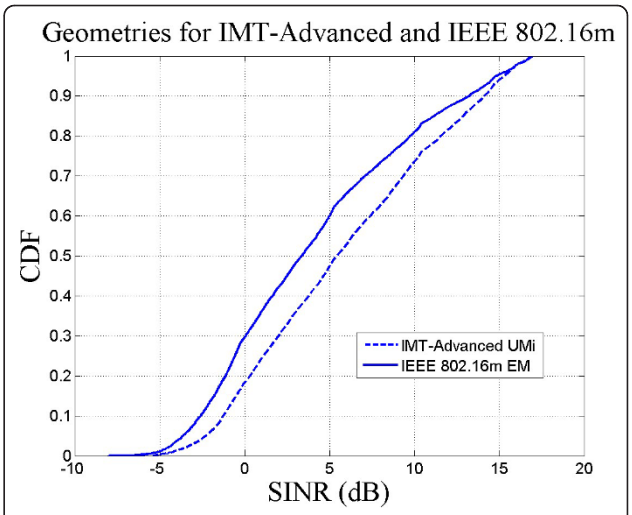

Figure 2 Geometries for the UMi test environment of IMT-Advanced and the IEEE 802.16 m evaluation methodology.

3. Dependence on the evaluation methodology

In a first step, the dependence of the performance of MU-MIMO on the evaluation methodology is investigated in this section. An 802.16 m system operating in the TDD mode with SLRU permutations and MU-MIMO as defined in Tables 2 and 3 of the Appendix is assumed to be the target mobile broadband system in this article. All simulation results in this section assume the 4 × 2 antenna configuration in the downlink. The system is evaluated for both the UMi test environment of the IMT-Advanced evaluation methodology and the IEEE 802.16 m evaluation methodology. Regarding the IEEE 802.16 m evaluation methodology, the ITU PB3 channel model is assumed with a Laplacian angular power profile at the BS of three degrees angular spread (AS). Unlike the IMT-Advanced evaluation methodology, the geometries, also referred to as the SINR cumulative distribution functions (CDFs) [16], are independent of the channel model and user speed in the IEEE 802.16 m evaluation methodology. Figure 2 shows the geometries of the investigated deployment scenarios of this section. Owing to the different models regarding the LSPs, an appreciable difference in favor of the UMi test environment is observed in Figure 2 regarding the SINR CDF. However, since the UMi test environment has significantly higher AS, see [11], it is expected that the MU-MIMO ZF transmission at the BS will appear more beneficial for the IEEE 802.16 m test scenario with respect to both processes of MU-MIMO pairing and interference generation. In order to calculate the average and cell-edge user spectral efficiencies which will assess the impact of both long-term and short-term channel model statistics on the system performance, the control overhead calculation needs to first take place. Table 4 presents the calculations for the considered deployment scenarios of this section according to the guidelines provided in Section 2.4. In the investigated TDD mode with 20 MHz channel bandwidth, 31:19 DL:UL ratio, and 1/16 CP length, see Table 4, the total number of LRUs equals 496 and the total number of OFDMA symbols in the DL portion of the TDD frame equals 31.

The control overhead in Table 4 is expressed in both LRUs or symbols and percentage of the total resources. As shown in Table 4, there are more user allocations in the case of the IEEE 802.16 m test scenario because the A-A-MAP overhead is higher than the one in the UMi test environment of IMT-Advanced. However, the overall control overhead does not differ significantly between the two cases since most of the overhead is contributed from the fixed control signaling part. It is noted that similar calculations were performed in [17] for the IMT-Advanced UMi test environment.

In order to make the final assessment on the impact of the evaluation methodology on the MU-MIMO system performance, Figure 3 shows the user throughput CDFs for the investigated deployment scenarios.

Figure 3 shows that despite the initial geometry advantage of the IMT-Advanced UMi test environment over the considered test scenario of the IEEE 802.16 m evaluation methodology, see Figure 2, the latter offers superior performance with respect to both average and cell-edge user spectral efficiencies. The main reason for this effect lies in the difference between the AS of the IMT-Advanced UMi test environment and the assumed AS of three degrees of the IEEE 802.16 m evaluation methodology: When the AS is small, not only the BF gains are higher but also–more

Table 4 DL control overhead for the considered deployment scenarios of Section 3

	IMT-Advanced UMi test environment		IEEE 802.16 m test scenario, ITU PB3, 3 degree AS	
	Overhead in LRUs or symbols	Overhead in %	Overhead in LRUs or symbols	Overhead in %
DL A-A-map	16.6 LRUs	3.35	19.4 LRUs	3.91
DL A-A-map	8.1 LRUs	1.63	9.5 LRUs	1.92
HF-A-map	1 LRU	0.20	1 LRU	0.20
NUS-A-map	3.75 LRUs	0.76	3.75 LRUs	0.76
A-preamble	1 symbol	3.23	1 symbol	3.23
A-midamble	1 symbol	3.23	1 symbol	3.23
SFH	5 LRUs	1.01	5 LRUs	1.01
Total overhead		13.41%		14.26%

importantly for MU-MIMO operation–MU-MIMO pairing becomes more efficient since lower inter-user interference can be achieved, i.e., there is higher probability to identify MU-MIMO pairs which have lower inter-user interference in the case of small AS. The spectral efficiency results are summarized in Table 5. It is noted that the results in Figure 3 and Table 5 explicitly consider the impact of the control overhead calculations according to Table 4. As revealed in Table 5, the gains are high for both the average and cell-edge user spectral efficiencies which show the substantial benefits of MU-MIMO with ZF transmission in the case of highly directional propagation environments. Since the information in Table 5 sufficiently conveys the conclusions from the user throughput CDFs in Figure 3, system-level simulation results are presented in the format of Table 5 for the remainder of the article.

4. Dependence on deployment parameters

After illustrating the impact of the evaluation methodology on the spectral efficiency of a mobile broadband MU-MIMO system such as IEEE 802.16 m, this section discusses the impact of different deployment parameters on the performance of MU-MIMO. First, the impact of different deployment scenarios is investigated in Section 4.1 for both considered evaluation methodologies. Section 4.2 deals with another critical component of a mobile broadband deployment which is the antenna configuration used at the BS sites by investigating the influence of the number of transmit ($T \times$) antennas per sector and antenna spacing on the performance of MU-MIMO.

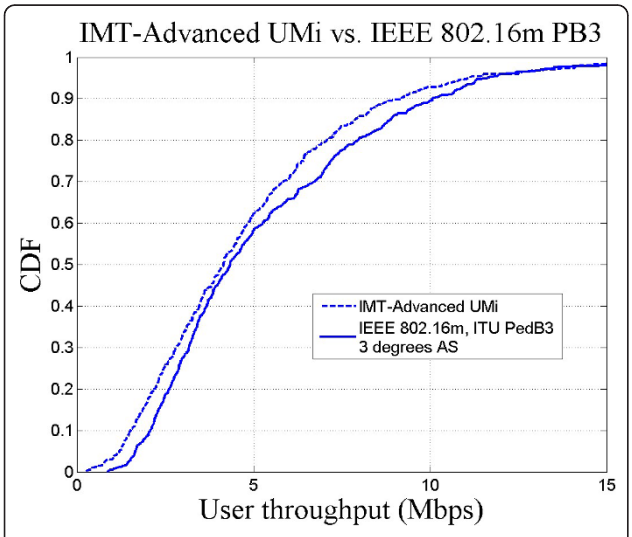

Figure 3 User throughput CDFs for the UMi test environment of IMT-Advanced and the IEEE 802.16 m PB3 and 3 degrees AS.

4.1. Deployment scenarios

In this section, the impact of different deployment scenarios on the performance of MU-MIMO is investigated. All the results in this section assume the 4 × 2 antenna configuration with λ/2 antenna spacing at both BS and MS. In a first step, the three test environments of the IMT-Advanced evaluation methodology are considered. Then, the results for all the three channel models of the IEEE 802.16 m evaluation methodology, i.e., ITU PB3, ITU VA30, and ITU VA120, are presented. The impact of the value of the AS is also considered in the case of the IEEE 802.16 m evaluation methodology.

Figure 4 shows the geometries for all the three test environments of the IMT-Advanced evaluation methodology considered in this article, i.e., UMi, UMa, and RMa. Table 6 presents the sector/cell-edge user throughput and the corresponding spectral efficiencies for all the three test environments assuming that IEEE 802.16 m operates in the TDD mode (see Table 2 of the Appendix) with MU-MIMO and SLRU permutations in the case of the UMi test environment and MU-MIMO with NLRU permutations in the case of the UMa and RMa test environments (see Table 3 of the Appendix).

Since the SINR distributions of the UMa and UMi test environments are similar (see Figure 4) and UMa has higher user mobility (30 km/h) compared to UMi (3 km/h), it is reasonable to expect that the performance of the UMa test environment is degraded compared to the performance of the UMi test environment. One

Table 5 Summary of the system-level simulation results for the considered deployment scenarios of Section 3

	IMT-Advanced UMi test environment	IEEE 802.16 m test scenario, ITU PB3, 3 degree AS
Average sector throughput	44.08 Mbps	48.25 Mbps
Average spectral efficiency	3.55 b/s/Hz/sector	3.89 b/s/Hz/sector
Cell-edge user throughput	999 Kbps	1392 Kbps
Cell edge-user spectral efficiency	0.081 b/s/Hz/user	0.112 b/s/Hz/user

would expect that the spectral efficiency would further reduce for the RMa test environment because of the higher mobility of 120 km/h as compared to the UMa test environment (30 km/h). However, the simulation results reveal better performance than the UMa for both the cell and cell-edge user spectral efficiencies. This effect can be explained by the following observations:

- The carrier frequency of RMa is 800 MHz (see Table 1), which leads to a Doppler frequency of 88.9 Hz. If we compare the Doppler frequency of RMa with that of the UMa test environment, which is 55.6 Hz (30 km/h at 2 GHz carrier frequency), see also Table 1, we can observe that the difference is not significant. As a result, the performance degradation due to channel/sounding estimation and feedback delay errors is not expected to be substantial.
- If the SINR distributions in Figure 4 are compared, a consistent SINR gain ranging from 0.75 to 1 dB is observed for the RMa test environment for the greater part of the SINR distribution, e.g., from the 5th to the 80th percentile, while the gain is consistent, albeit lower, for the rest of the distribution. The observed SINR gain, which is valid for both cell-edge and cell-center users in the network, can offset the slight performance degradation because of the higher Doppler speed in the RMa test environment compared to UMa.
- There is higher probability for line-of-sight (LOS) links in the RMa test environment compared to the UMa test environment because of the higher distances expected to be encountered in the RMa test environment, see Table 1 in this article as well as Table Aone-three of Annex 1 in [1]. In addition to the improvement in the geometry, this effect seems to lead to higher BF gains for the RMa test environment as well as more favorable MU-MIMO ZF operation compared to UMa.

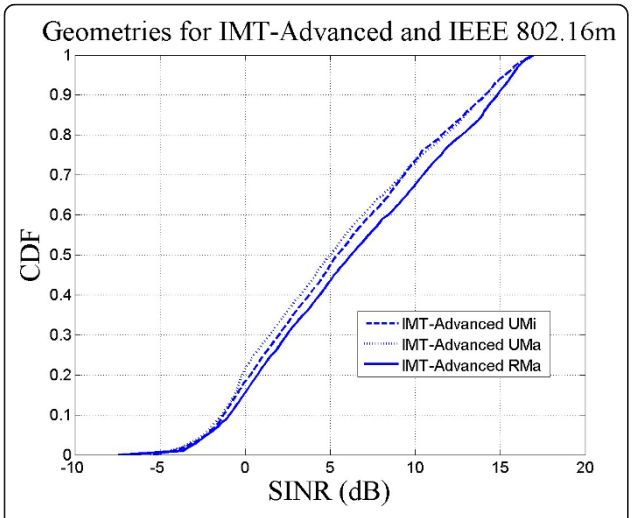

Figure 4 Geometries for the UMi, UMa, and RMa test environments of the IMT-Advanced evaluation methodology.

The results of Table 6 indicate that the user mobility is not necessarily the determining factor for assessing the performance of a mobile broadband deployment. The combination of the carrier frequency, geometry, and spatial profile, e.g., probability of LOS and angular spread, need to be explicitly considered in order to gain insight into the performance of a MU-MIMO mobile broadband system. Given the superiority of RMa over both UMi and UMa test environments according to the results of Table 6 as well as the superiority of ITU PB3 over UMi according to the results of Table 5 in Section 3, it becomes apparent that the spatial profile of the considered deployment scenario plays a fundamental role in MU-MIMO systems operating with ZF transmission at the BS. It is noted that the results presented in Table 6 correlate well with corresponding results from [17] for IEEE 802.16 m.

In the remainder of this section, system-level simulation results are presented for the IEEE 802.16 m evaluation methodology for all three channel models, i.e., ITU PB3, ITU VA30, and ITU VA120. As already mentioned in Section 3, there is a single geometry for all three channel models of the baseline test scenario of the IEEE 802.16 m evaluation methodology adopted in this article (see Figure 1). Therefore, the results in Table 7 serve the purpose of investigating the impact of mobility on the MU-MIMO performance. The system parameters of IEEE 802.16 m for the three scenarios of 3, 30, and 120 km/h correspond to the system parameters in Table 6 for UMi, UMa, and RMa which assume user speeds of 3, 30, and 120 km/h, respectively.

As shown in Table 7 mobility has a clear impact on the MU-MIMO performance in the case that the

Table 6 System-level simulation results for the considered test environments of IMT-Advanced

	UMi test environment	UMa test environment	RMa test environment
Average sector throughput	44.08 Mbps	33.48 Mbps	45.63 Mbps
Average spectral efficiency	3.55 b/s/Hz/sector	2.70 b/s/Hz/sector	3.68 b/s/Hz/sector
Cell-edge user throughput	999 Kbps	818 Kbps	1091 Kbps
Cell edge-user spectral efficiency	0.081 b/s/Hz/user	0.066 b/s/Hz/user	0.088 b/s/Hz/user

underlying carrier frequency and LSPs are the same: There is a clear advantage in low mobility scenarios which benefit from the use of frequency-selective scheduling with SLRU [16]. As the user speed increases from 3 to 30 km/h, i.e., the Doppler frequency increases by ten times, both average and cell-edge user spectral efficiencies decrease by 21.6 and 36.6%, respectively. The additional increase from 30 to 120 km/h does not seem to have an additional detrimental effect on the spectral efficiencies. In fact, the increased diversity achieved at higher mobility seems to offset the performance degradation because of feedback delays and estimation errors.

The investigations in this section conclude with the impact of the AS on the MU-MIMO performance. Table 8 presents the results for the IEEE evaluation methodology when the AS is 15 degrees. The rest of the parameters are identical to the parameters used for generating the results in Table 7.

If we compare the results in Table 7 (3 degrees AS) with the ones in Table 8 (15 degrees AS), we observe a consistent performance degradation as the AS increases. Interestingly enough, the performance degradation is relatively similar across the different channel models for both average and cell-edge user spectral efficiencies, which reveals that the impact of a larger AS value on the performance of MU-MIMO is essentially independent from the mobility scenario and exhibits similar relative degradation for both average and cell-edge user spectral efficiencies.

4.2. Antenna configuration

In this section, the impact of the antenna configuration used at the BS sectors on the performance of MU-MIMO is investigated. Table 9 presents the simulation results for the 2 × 2 antenna configuration with λ/2 antenna spacing using the IEEE 802.16 m evaluation methodology. The comparison of the results in Table 9 with Table 7 (λ/2 antenna spacing for both) shows the dramatic improvement of both average and cell-edge user performances when four T × antennas are used at the BS sector transmitter. The improvement of the average spectral efficiency exceeds 50% for the low mobility scenario (ITU PB3) and is on the order of 65% for the medium (ITU VA30) and high mobility (ITU VA120) cases. The situation is extremely favorable also for the cell-edge user spectral efficiency which exhibits improvements from approximately 42% for ITU VA120 to 54% for ITU PB3. Those results clearly indicate that the use of four T × antennas per sector at the BS sites of next-generation mobile broadband systems is highly desirable because of the significant MU-MIMO performance benefits which stem not only from the higher BF gain, but also from the opportunity to schedule up to four simultaneous MU-MIMO users per allocation with four T × antennas, see Table 3 of the Appendix and [16].

Table 10 presents the simulation results with 4λ antenna spacing using the IMT-Advanced evaluation methodology. The comparison of the results in Table 10 (4 × 2 antenna configuration, 4λ antenna spacing) with Table 6 (4 × 2 antenna configuration, λ/2 antenna spacing) shows the impact of the antenna spacing depending not only on the test environment, but also on the performance metric. More specifically, although the gains with smaller antenna spacing (λ/2) are moderate for the UMi test environment, 2.8 and 10.5% for the average and cell-edge user spectral efficiencies, respectively, they are significantly higher for both UMa and RMa, 15.7 and 23.7% on the average for the average and cell-edge user spectral efficiencies, respectively. Since the investigated deployment scenarios span a wide range with respect to LSPs/channel models, carrier frequencies, and user mobility profiles, it can be concluded that the use of λ/2 antenna spacing at the BS antenna array is associated with significant benefits for the

Table 7 System-level simulation results for the IEEE 802.16 m evaluation methodology, 3 degrees AS

	ITU PB3	ITU VA30	ITU VA120
Average sector throughput	48.25 Mbps	37.82 Mbps	38.69 Mbps
Average spectral efficiency	3.89 b/s/Hz/sector	3.05 b/s/Hz/sector	3.12 b/s/Hz/sector
Cell-edge user throughput	1392 Kbps	880 Kbps	918 Kbps
Cell edge-user spectral efficiency	0.112 b/s/Hz/user	0.071 b/s/Hz/user	0.074 b/s/Hz/user

Table 8 System-level simulation results for the IEEE 802.16 m evaluation methodology, 15 degrees AS

	ITU PB3	ITU VA30	ITU VA120
Average sector throughput	45.11 Mbps	34.30 Mbps	35.30 Mbps
Average spectral efficiency	3.64 b/s/Hz/sector	2.77 b/s/Hz/sector	2.85 b/s/Hz/sector
Cell-edge user throughput	1,310 Kbps	790 Kbps	818 Kbps
Cell edge-user spectral efficiency	0.106 b/s/Hz/user	0.064 b/s/Hz/user	0.066 b/s/Hz/user

performance of MU-MIMO with ZF in a wide range of propagation environments.

5. Dependence on system parameters

After showing in Section 4 the impact of different deployment parameters on the performance of MU-MIMO, this section presents the dependence of the MU-MIMO performance on a number of system parameters which are expected to play an important role in the successful deployment of mobile broadband MU-MIMO systems such as IEEE 802.16 m. The considered parameters are the duplex mode, permutations, amount of feedback from the MS to the BS, and sounding, channel estimation, and control signaling errors. The results of this section provide a means for appreciating the impact of the considered parameters and also, wherever possible, deciding on their values in practical MU-MIMO deployments.

5.1. Duplex mode (TDD/FDD)

The system-level simulation results presented in Sections 3 and 4 assume TDD operation for the target IEEE 802.16 m mobile broadband system with MU-MIMO. In the section, the results for FDD are presented using the IMT-Advanced evaluation methodology. For a fair comparison, the total amount of spectrum used in the case of the 2 × 10 MHz FDD configuration (see Table 11) is equal to the total amount of spectrum used by the 20 MHz TDD system, see Table 6. The comparison of the FDD results in Table 11 with the TDD results in Table 6 shows that the performance of a MU-MIMO mobile broadband system does not critically depend on the duplex mode. The slightly higher overhead in the case of FDD compared to TDD for IEEE 802.16 m, see [16] for a detailed analysis, is offset by the presence of a DL/UL and UL/DL switching period in TDD–equal to one OFDMA symbol–where no information is transmitted. Therefore, the selection of the duplex mode is not critical for MU-MIMO operation, i.e., MU-MIMO works equally well in both FDD and TDD mobile broadband system deployments.

5.2. Permutations

As mentioned in Section 2.3, there is a synergy between the used subchannelization, MU-MIMO operation, and MS feedback requirements. This section shows how the performance of MU-MIMO is affected by the selection of subchannelization in different deployment scenarios. Table 12 compares the performance of SLRU and NLRU permutations in all three IMT-Advanced test environments considered in this article. According to the results in Table 12 for the UMi test environment, the significant benefits of SLRU permutations–and the associated frequency-selective scheduling they enable–over the NLRU permutation are shown especially for the cell-edge user performance. The situation is reversed for the higher mobility test environments (UMa and RMa) where the NLRU subchannelization scheme outperforms the SLRU subchannelization scheme with respect to both average and cell-edge user spectral efficiencies. Although the gains of NLRU over SLRU in UMa and RMa are somewhat reduced with respect to the cell-edge user performance compared to the gains of SLRU over NLRU in UMi, the choice on NLRU for higher mobility propagation environments is still justified according to Table 12. Those results provide clear insights into the performance tradeoffs in selecting SLRU or NLRU permutations for different deployment scenarios and can be used by the mobile broadband network designer to choose the appropriate subchannelization scheme for MU-MIMO deployments with specific mobility and average/cell-edge user performance targets.

5.3. CQI/PMI feedback quantity

As described in Section 2.2, the use of the SLRU permutations is associated with allocation-dependent CQI and

Table 9 System-level simulation results for the IEEE 802.16 m evaluation methodology, 2 × 2 antenna configuration

	ITU PB3	ITU VA30	ITU VA120
Average sector throughput	31.74 Mbps	22.82 Mbps	23.44 Mbps
Average spectral efficiency	2.56 b/s/Hz/sector	1.84 b/s/Hz/sector	1.89 b/s/Hz/sector
Cell-edge user throughput	905 Kbps	595 Kbps	645 Kbps
Cell edge-user spectral efficiency	0.073 b/s/Hz/user	0.048 b/s/Hz/user	0.052 b/s/Hz/user

Table 10 System-level simulation results for the IMT-Advanced evaluation methodology, 4λ antenna spacing

	UMi test environment	UMa test environment	RMa test environment
Average sector throughput	42.90 Mbps	28.40 Mbps	40.18 Mbps
Average spectral efficiency	3.46 b/s/Hz/sector	2.29 b/s/Hz/sector	3.24 b/s/Hz/sector
Cell-edge user throughput	904 Kbps	655 Kbps	890 Kbps
Cell edge-user spectral efficiency	0.073 b/s/Hz/user	0.053 b/s/Hz/user	0.072 b/s/Hz/user

TCI feedback from the MS to the BS which enables frequency-selective scheduling. All the results presented in Tables 5, 6, 7, 8, 9, 10, 11 and 12 for SLRU assume full CQI and TCI feedback from the MS which is translated into 12 CQI and TCI values for the target IEEE 802.16 m mobile broadband system. In this section, the impact of limited CQI and TCI feedback on the MU-MIMO performance is investigated for the UMi test environment of IMT-Advanced. Table 13 presented the system-level simulation results for different levels of CQI and TCI feedback using the Best-*M* notation [18], where *M* takes the values 3, 4, 6, 9, and 12 (full CQI/TCI feedback as in Table 6 for UMi). Although the performance degradation of the cell-edge user spectral efficiency does not exceed 5% for Best-4 to Best-9, the average sector throughput and spectral efficiency are significantly impacted by the use of limited CQI and TCI feedback with performance degradation up to 25% for Best-3. The results in Table 13 clearly indicate that deployments targeting high spectral efficiency MU-MIMO operation require increased amount of MS feedback.

5.4. Sounding, channel estimation, and control signaling errors

As a final investigation in Section 5, Table 14 presents system-level simulation results with and without error modeling for the UMi test environment of IMT-Advanced and the ITU PB3 channel model of the IEEE 802.16 m evaluation methodology. There are three types of errors modeled in the system-level simulations: Downlink channel sounding errors which refer to the errors in determining the CQI and BF (TCI for SLRU and LT-PMI/LT-CM for NLRU) feedback when using the A-MIDAMBLE in IEEE 802.16 m, channel estimation errors which have different impact depending on the number of MU-MIMO users scheduled in a specific allocation and the correlation of their BF vectors, see also Section 2.3, and control signaling errors such as A-A-MAP, HF-A-MAP, and UL feedback channel transmission errors [16]. According to the results in Table 14, the impact of sounding, channel estimation, and control signaling errors is more pronounced for the UMi test environment than the ITU PB3 test scenario. Also, the impact is higher for the cell-edge user performance rather than the average spectral efficiency for both UMi and ITU PB3 deployment scenarios. Extensive simulation results have shown that channel estimation errors have bigger contribution to the performance degradation compared to channel sounding errors, whereas the impact of control signaling errors is much smaller.

6. The promise of MU-MIMO for technology evolution

In this section, the IEEE 802.16 m evaluation methodology with mixed mobility [12] is used for showing the advantages of the MU-MIMO technology for mobile broadband communications. Table 15 presents system-level simulation results for both IEEE 802.16e with SU-MIMO and IEEE 802.16 m with MU-MIMO. In both cases, the 2 × 2 and 4 × 2 antenna configurations are used to show the additional benefits when four T × antennas are employed per sector at the BS. For a fair comparison, all technologies operate in the 10 MHz TDD mode. The IEEE 802.16e 2 × 2 system is an OL system with adaptive switching between space-time block coding (STBC) and SM [4,5]. The IEEE 802.16e 4 × 2 system uses UL channel sounding for acquiring wideband BF vectors which are applied to the DL STBC and SM transmission. According to the results of Table 15, the use of MU-MIMO offers a dramatic improvement of the spectral efficiency of IEEE 802.16 m compared to the spectral efficiency of IEEE 802.16e. Further, MU-MIMO ZF enables further performance advantages compared to SU-MIMO when four T × antennas are used at the BS. As a final remark, compared to a typical,

Table 11 System-level simulation results for the IMT-Advanced evaluation methodology, 2 × 10 MHz FDD

	UMi test environment	UMa test environment	RMa test environment
Average sector throughput	35.29 Mbps	27.10 Mbps	36.80 Mbps
Average spectral efficiency	3.53 b/s/Hz/sector	2.71 b/s/Hz/sector	3.68 b/s/Hz/sector
Cell-edge user throughput	838 Kbps	641 Kbps	880 Kbps
Cell edge-user spectral efficiency	0.084 b/s/Hz/user	0.064 b/s/Hz/user	0.088 b/s/Hz/user

Table 12 System-level simulation results for the IMT-Advanced evaluation methodology, comparison of SLRU and NLRU permutations for each test environment

	UMi		UMa		RMa	
	SLRU (from Table 6)	NLRU	NLRU (from Table 6)	SLRU	NLRU (from Table 6)	SLRU
Average sector throughput	44.08 Mbps	41.91 Mbps	33.48 Mbps	31.25 Mbps	45.63 Mbps	44.02 Mbps
Average spectral efficiency	3.55 b/s/Hz/sector	3.38 b/s/Hz/sector	2.70 b/s/Hz/sector	2.52 b/s/Hz/sector	3.68 b/s/Hz/sector	3.55 b/s/Hz/sector
Cell-edge user throughput	999 Kbps	818 Kbps	818 Kbps	806 Kbps	1,091 Kbps	1,029 Kbps
Cell edge-user spectral efficiency	0.081 b/s/Hz/user	0.066 b/s/Hz/user	0.066 b/s/Hz/user	0.065 b/s/Hz/user	0.088 b/s/Hz/user	0.083 b/s/Hz/user

Table 13 System-level simulation results for the UMi test environment of IMT-Advanced, comparison of amount of CQI/TCI feedback

	Best-3	Best-4	Best-6	Best-9	UMi results from Table 6
Average sector throughput	33.75 Mbps	34.65 Mbps	38.45 Mbps	41.77 Mbps	44.08 Mbps
Average spectral efficiency	2.72 b/s/Hz/sector	2.79 b/s/Hz/sector	3.10 b/s/Hz/sector	3.37 b/s/Hz/sector	3.55 b/s/Hz/sector
Cell-edge user throughput	905 Kbps	954 Kbps	954 Kbps	970 Kbps	999 Kbps
Cell edge-user spectral efficiency	0.073 b/s/Hz/user	0.077 b/s/Hz/user	0.077 b/s/Hz/user	0.078 b/s/Hz/user	0.081 b/s/Hz/user

Table 14 System-level simulation results to show the impact of sounding, channel estimation, and control signaling errors

	UMi		ITU PB3	
	Without errors	With errors (from Table 6)	Without errors	With errors (from Table 7)
Average sector throughput	47.99 Mbps	44.08 Mbps	47.72 Mbps	45.11 Mbps
Average spectral efficiency	3.87 b/s/Hz/sector	3.55 b/s/Hz/sector	3.85 b/s/Hz/sector	3.64 b/s/Hz/sector
Cell-edge user throughput	1,230 Kbps	999 Kbps	1505 Kbps	1,310 Kbps
Cell edge-user spectral efficiency	0.099 b/s/Hz/user	0.081 b/s/Hz/user	0.121 b/s/Hz/user	0.106 b/s/Hz/user

Table 15 System-level simulation results for the IEEE 802.16 m evaluation methodology, mixed mobility results, technology evolution

	IEEE 802.16e 2 × 2 SU-MIMO	IEEE 802.16e 4 × 2 SU-MIMO	IEEE 802.16 m 2 × 2 MU-MIMO	IEEE 802.16 m 4 × 2 MU-MIMO
Average sector throughput	8.00 Mbps	9.27 Mbps	14.14 Mbps	22.11 Mbps
Average spectral efficiency	1.30 b/s/Hz/sector	1.51 b/s/Hz/sector	2.28 b/s/Hz/sector	3.57 b/s/Hz/sector
Cell-edge user throughput	275 Kbps	375 Kbps	422 Kbps	626 Kbps
Cell edge-user spectral efficiency	0.045 b/s/Hz/user	0.061 b/s/Hz/user	0.068 b/s/Hz/user	0.101 b/s/Hz/user

current Mobile WiMAX deployment based on IEEE 802.16e with 2 × 2 SU-MIMO, an expected IEEE 802.16 m deployment with 4 × 2 MU-MIMO offers 2.8 times higher average spectral efficiency and 2.3 times higher cell-edge user spectral efficiency. Those gains are comparable to the gains achieved by 4 G systems such as Mobile WiMAX Release 1 and 3GPP LTE Release 8 over 3 G systems such as HSPA and clearly show that MU-MIMO is the appropriate technology for the evolution of 4 G MIMO OFDMA-based Mobile WiMAX Release 1 and 3GPP LTE Release 8 mobile broadband systems.

7. Conclusion

In this article, the benefits as well as the deployment and system parameter dependencies of the MU-MIMO technology are analyzed through an extensive simulation study for a next-generation mobile broadband system such as IEEE 802.16 m. A multitude of deployment scenarios and system parameters are investigated based on

widely used system-level evaluation methodologies. The results clearly indicate that user mobility is not necessarily the determining factor for assessing the performance of a mobile broadband deployment. The combination of carrier frequency, geometry, and spatial profile, e.g., probability of LOS and angular spread, needs to be explicitly considered for gaining insight into the performance of a MU-MIMO mobile broadband system. Further, it is shown that the use of four transmit antennas per sector at the BS sites of next-generation mobile broadband systems is highly desirable because of their significant MU-MIMO performance benefits compared to the deployment of two transmit antennas. Also, the results indicate that the use of closely spaced elements at the BS antenna array is associated with significant benefits for the performance of MU-MIMO. The results of this article can be used by the mobile broadband network designer for maximizing the benefits of MU-MIMO in a scenario with specific deployment requirements and goals by selecting the appropriate system parameters related to MU-MIMO after a close consideration of the different performance and implementation tradeoffs.

Appendix

In this appendix, the detailed assumptions of the IEEE 802.16 m downlink are given. The main OFDMA and frame parameters of IEEE 802.16 m are listed in Table 2, see also [13] and the companion documents [14,15]. Table 3 lists the main downlink system parameters of IEEE 802.16 m according to [13-16].

Competing interests

The authors declare that they have no competing interests.

Received: 1 December 2010 Accepted: 16 August 2011
Published: 16 August 2011

References

1. Informa Telecoms and Media, "Mobile Internet Traffic: Analyzing Global Usage Trends", http://media2.telecoms.com/downloads/mobile-internet-traffic-trends.pdf (2010)
2. Cisco, "Visual Networking Index: Global Mobile Data Traffic Forecast Update, 2009-2014", http://www.cisco.com/en/US/solutions/collateral/ns341/ns525/ns537/ns705/ns827/white_paper_c11-520862.html (2010)
3. D Gesbert, M Kountouris, RW Heath Jr, C-B Chae, T Saelzer, From single-user to multi-user communications: shifting the MIMO paradigm. IEEE Signal Process Mag. **24**(5), 36–36 (2007)
4. A Davydov, R Srinivasan, S Timiri, Y-S Choi, H Yin, A Salvekar, A Papathanassiou, MIMO spectral efficiency of the Mobile WiMAX downlink. *Mobile WiMAX: Toward Broadband Wireless Metropolitan Area Networks*, ed. by Zhang Y, Chen H-H (Auerbach Publications, Taylor & Francis Group (2007)
5. R Srinivasan, S Timiri, A Davydov, A Papathanassiou, Downlink spectral efficiency of Mobile WiMAX, in *IEEE Vehicular Technology Conference (VTC Spring 2007)*, Dublin, Ireland, 2786–2790 (2007)
6. WiMAX Forum, "WiMAX, HSPA+, and LTE: A comparative Analysis", Whitepaper, http://www.wimaxforum.org/sites/wimaxforum.org/files/document_library/wimax_hspa+and_lte_111809_final.pdf (November 2009)
7. Q Spencer, AL Swindlehurst, M Haardt, Zero-forcing methods for downlink spatial multiplexing in multiuser MIMO channels. IEEE Trans Signal Process. **52**(2), 462–471 (2004)
8. L Sanguinetti, HV Poor, Fundamentals of multi-user MIMO communications. *New Directions in Wireless Communications Research*, Springer, ed. by Tarokh V (2009)
9. A Paulraj, R Nabar, D Gore, *Introduction to Space-Time Communications* (Cambridge University Press, 2003)
10. G Morozov, A Davydov, A Papathanassiou, A novel combined CSI feedback mechanism to support multi-user MIMO beamforming schemes in TDD-OFDMA systems, in *1st International Workshop on Recent Advances in Broadband Access Networks Conference (RABAN 2010)*, (2010)
11. Report ITU-R M.2135-1, Guidelines for evaluation of radio interface technologies for IMT-Advanced, (February 2010)
12. IEEE 802.16 m-08/004r5, IEEE 802.16m Evaluation Methodology Document (EMD), (January 2009)
13. IEEE Std 802.16-2009, IEEE Standard for Local and metropolitan area networks—Part 16: Air Interface for Broadband Wireless Access Systems
14. IEEE 802.16m-07/002, IEEE 802.16m System Requirements Document (SRD)
15. IEEE 802.16m-09/0034, IEEE 802.16m System Description Document (SDD)
16. A Papathanassiou *et al.*, IEEE 802.16m evaluation results for the PCT of IMT-dvanced, document IEEE C802.16-0013 (September 2009)
17. Document IMT-ADV/15-E, Evaluation of IMT-Advanced Candidate Technology Submissions in Documents IMT-ADV/4 and IMT-ADV/8, Russian Evaluation Group, http://www.itu.int/md/R07-IMT.ADV-C-0015/en (July 2010)
18. J Leinonen, J Hamalainen, M Juntti, Outage capacity analysis of resource allocation mechanisms in downlink MIMO-OFDMA systems with best-M feedback method, in *IEEE 10th Workshop on Signal Processing Advances in Wireless Communications 2009 (SPAWC'09)*, 146–150 (2009)

doi:10.1186/1687-1499-2011-63
Cite this article as: Papathanassiou and Davydov: **The promise of downlink MU-MIMO for high-capacity next generation mobile broadband networks based on IEEE 802.16 m.** *EURASIP Journal on Wireless Communications and Networking* 2011 **2011**:63.